J|A|C|S
ARTICLES
Published on Web 09/06/2003

Probing Residual Interactions in Unfolded Protein States Using NMR Spin Relaxation Techniques: An Application to Δ131Δ

Wing-Yiu Choy* and Lewis E. Kay*

Contribution from the Protein Engineering Network Centers of Excellence and Departments of Medical Genetics and Microbiology, Biochemistry, and Chemistry, University of Toronto, Toronto, Ontario, Canada M5S 1A8

Received April 18, 2003; E-mail: kay@pound.med.utoronto.ca; choy@pound.med.utoronto.ca

Abstract: Residual interactions in Δ131Δ, a large disordered fragment of staphylococcal nuclease, have been probed at two different pHs using backbone ^{15}N and side-chain methyl ^{2}H NMR spin relaxation techniques. The amplitudes of picosecond time-scale motions of both the backbone and side chains do not change considerably at either pH value, although they are significantly larger than those observed for folded proteins. In contrast, dramatic increases in the amplitudes of motions occurring on a nanosecond time scale are observed throughout Δ131Δ at pH 3 relative to pH 5. This is consistent with a picture in which residual hydrophobic contacts at pH 5 are disrupted by electrostatic repulsions that dominate at the lower pH.

Introduction

A significant number of protein sequences are predicted to code for unstructured conformations,[1] and recent experimental results have indeed confirmed that many functional proteins are intrinsically disordered under physiological conditions.[2−4] Structural characterization and dynamic studies of these proteins will lead to a better understanding of how they function, which is critical since most are involved in important cell regulatory events. In addition, such studies will shed light on the protein folding problem.

NMR is a powerful technique for studying disordered states of proteins at atomic resolution, and recently developed multidimensional NMR methods have made a significant impact on the characterization of residual structure in such systems.[5,6] A disordered state ensemble, however, cannot be completely described without knowledge of its dynamical properties. Because ^{15}N chemical shifts are, in general, well dispersed in unfolded proteins, amide ^{15}N relaxation measurements are commonly employed to probe backbone dynamics on a per-residue basis.[7] Complementary information in the form of side chain dynamics is also of interest, and our laboratory has recently developed methodology to measure ^{2}H spin relaxation rates at side chain $^{13}CH_2D$ methyl positions in ^{15}N,^{13}C-labeled and fractionally deuterated samples of unfolded proteins.[8,9] The dynamics of methyl-containing side chains have been measured in Δ131Δ, one of several model systems used to study unfolded states of proteins.[9] Δ131Δ, a large fragment of wild-type staphylococcal nuclease (deletion of wild-type residues 3−12 and 141−149), is unfolded under nondenaturing conditions (pH $\approx$ 5 and low salt concentration). Extensive structural characterization of this protein has been carried out using NMR and other spectroscopic techniques. Experimental data such as backbone relaxation rate measurements and paramagnetic relaxation enhancement of amide protons clearly establish the presence of a significant amount of residual structure.[10−13] Of interest, our dynamics study at pH 5 shows a good correlation between the amplitudes of motion of the methyl symmetry axis and backbone ^{1}H−^{15}N bond vectors within the same residue.[9] A simple model, the cone−Gaussian-axial-fluctuation (cone−GAF) model, was developed that allows extraction of the amplitudes of χ_1 torsion angle fluctuations ($\sigma_{\chi 1}$) for valine and threonine residues. On the basis of this model, $\sigma_{\chi 1}$ values for the six valine residues for which data could be obtained were estimated to be on average 10° larger than in folded proteins.[9]

The presence of a significant amount of residual structure in Δ131Δ at pH 5 raises the question of how it affects the measured dynamics. That is, to what extent do backbone and side chain dynamics report on these residual interactions, and how would

(1) Dunker, A. K.; Lawson, J. D.; Brown, C. J.; Williams, R. M.; Romero, P.; Oh, J. S.; Oldfield, C. J.; Campen, A. M.; Ratliff, C. M.; Hipps, K. W.; Ausio, J.; Nissen, M. S.; Reeves, R.; Kang, C. H.; Kissinger, C. R.; Bailey, R. W.; Griswold, M. D.; Chiu, W.; Garber, E. C.; Obradovic, Z. *J. Mol. Graph. Model.* **2001**, *19*, 26−59.
(2) Kriwacki, R. W.; Hengst, L.; Tennant, L.; Reed, S. I.; Wright, P. E. *Proc. Natl. Acad. Sci. U.S.A.* **1996**, *93*, 11504−11509.
(3) Campbell, K. M.; Terrell, A. R.; Laybourn, P. J.; Lumb, K. J. *Biochemistry* **2000**, *39*, 2708−2713.
(4) Nash, P.; Tang, X.; Orlicky, S.; Chen, Q.; Gertler, F. B.; Mendenhall, M. D.; Sicheri, F.; Pawson, T.; Tyers, M. *Nature* **2001**, *414*, 514−521.
(5) Shortle, D.; Wang, Y.; Gillespie, J. R.; Wrabl, J. O. *Protein Sci.* **1996**, *5*, 991−1000.
(6) Dyson, H. J.; Wright, P. E. *Nat. Struct. Biol.* **1998**, supplement, 499−503.
(7) Farrow, N. A.; Zhang, O. W.; Forman-Kay, J. D.; Kay, L. E. *Biochemistry* **1995**, *34*, 868−878.
(8) Muhandiram, D. R.; Johnson, P. E.; Yang, D.; Zhang, O.; McIntosh, L. P.; Kay, L. E. *J. Biomol. NMR* **1997**, *10*, 283−288.
(9) Choy, W. Y.; Shortle, D.; Kay, L. E. *J. Am. Chem. Soc.* **2003**, *125*, 1748−1758.
(10) Alexandrescu, A. T.; Shortle, D. *J. Mol. Biol.* **1994**, *242*, 527−546.
(11) Gillespie, J. R.; Shortle, D. *J. Mol. Biol.* **1997**, *268*, 158−169.
(12) Gillespie, J. R.; Shortle, D. *J. Mol. Biol.* **1997**, *268*, 170−184.
(13) Ackerman, M. S.; Shortle, D. *Biochemistry* **2002**, *41*, 3089−3095.

10.1021/ja035705q CCC: $25.00

Table 1. Motional Parameters of Side Chain Methyl Rotation Axes Extracted Using the LS-3 Spectral Density Model[14−17]

	pH 5.1			pH 3.1			Δ[c]	
residue	S^2_{axis}	τ_f (ps)	τ_c^{eff} (ns)	S^2_{axis}	τ_f (ps)	τ_c^{eff} (ns)	ΔS^2_{axis}	$\Delta\tau_c^{eff}$ (ns)
V51	0.21 ± 0.02	44 ± 2	3.0 ± 0.2	0.18 ± 0.01	41 ± 0.3	2.5 ± 0.1	0.03 ± 0.02	0.5 ± 0.2
V66	0.27 ± 0.03	49 ± 2	4.7 ± 0.6	*a*	*a*	*a*	*a*	*a*
V74	0.34 ± 0.03	52 ± 3	4.9 ± 0.4	0.33 ± 0.02	43 ± 1	3.5 ± 0.3	0.01 ± 0.04	1.4 ± 0.5
V104	0.50 ± 0.09	52 ± 7	5.4 ± 1.1	*a*	*a*	*a*	*a*	*a*
V111	0.30 ± 0.04	49 ± 3	5.4 ± 0.6	0.33 ± 0.03	42 ± 2	2.4 ± 0.3	−0.03 ± 0.05	3.0 ± 0.7
V114	0.34 ± 0.04	49 ± 3	5.5 ± 0.6	0.35 ± 0.02	44 ± 1	2.8 ± 0.1	−0.01 ± 0.04	1.7 ± 0.6
T62	0.32 ± 0.03	57 ± 2	5.1 ± 0.4	*a*	*a*	*a*	*a*	*a*
T82	–	–	–	0.31 ± 0.03	53 ± 2	3.5 ± 0.3	a	a
T120	0.32 ± 0.03	49 ± 3	3.0 ± 0.3	*a*	*a*	*a*	*a*	*a*
A58	0.39 ± 0.01	43 ± 1	4.1 ± 0.1	0.31 ± 0.01	42 ± 0.2	3.2 ± 0.1	0.08 ± 0.01	0.9 ± 0.2
A60	0.38 ± 0.01	48 ± 1	4.9 ± 0.2	0.32 ± 0.05	43 ± 0.3	3.6 ± 0.1	0.06 ± 0.05	1.3 ± 0.2
A102	0.83 ± 0.07	42 ± 6	5.4 ± 0.5	*a*	*a*	*a*	*a*	*a*
A112	0.54 ± 0.05	46 ± 4	6.1 ± 0.6	0.39 ± 0.09	43 ± 0.4	4.3 ± 0.1	0.15 ± 0.10	1.8 ± 0.6
A130	0.31 ± 0.02	47 ± 2	3.0 ± 0.2	0.26 ± 0.05	44 ± 0.2	2.5 ± 0.1	0.05 ± 0.05	0.5 ± 0.2
I72	0.38 ± 0.04	25 ± 5	5.2 ± 0.6	*a*	*a*	*a*	*a*	*a*
I139	0.14 ± 0.02	31 ± 2	3.6 ± 0.5	0.14 ± 0.01	28 ± 1	2.1 ± 0.1	0.00 ± 0.02	1.5 ± 0.8
L108	0.22 ± 0.04	34 ± 4	6.6 ± 1.6	*a*	*a*	*a*	*a*	*a*
L137	0.15 ± 0.02	34 ± 2	2.6 ± 0.4	*b*	*b*	*b*	*a*	*a*

[a] Data not available. [b] The ^{2}H relaxation rates could not be well fit using the LS-3 model. [c] Δ: $\Delta X = X$ (pH 5) − X (pH 3).

such motions change in a "more completely denatured state" with fewer contacts? To investigate this we have measured ^{15}N backbone and methyl ^{2}H side chain relaxation properties (including ^{15}N R_1, $R_{1\rho}$ rates and steady-state ^{1}H−^{15}N NOE values, longitudinal (D_z), transverse (D_+), anti-phase transverse (D_+D_z+D_zD_+) and quadrupolar ($3D_z^2 - 2$) rates) for Δ131Δ at pH 3, where many of these remaining contacts are removed, and compared these values to those obtained at pH 5 (ref 9). The data are consistent with little change in the magnitude of picosecond (ps) time-scale dynamics but significant increases in motions occurring on a nanosecond (ns) time scale as the pH is dropped, likely reflecting the disruption of residual hydrophobic contacts due to electrostatic repulsion at the lower pH.

Results and Discussion

Dynamics parameters of the backbone and methyl side chains (pH 5 and 3) have been obtained by fitting the backbone ^{15}N and side chain ^{2}H relaxation rates to a modified Lipari−Szabo model (LS-3 model).[9,10,14−16] The model employs a spectral density function of the form,

$$J(\omega) = \frac{\alpha S_f^2 \tau_c^{eff}}{1 + (\omega\tau_c^{eff})^2} + \frac{(1 - \alpha S_f^2)\tau}{1 + (\omega\tau)^2}$$

with

$$1/\tau = 1/\tau_c^{eff} + 1/\tau_f \quad (1)$$

In eq 1 the value of α is set to 1 and 1/9 in the analysis of ^{15}N and ^{2}H spin relaxation data, respectively, S_f^2 is an order parameter which provides a measure of the amplitude of the fast (ps) dynamics of the ^{15}N−^{1}H bond vector or methyl three-fold axis, τ_f is the correlation time of this motion, and τ_c^{eff} is a residue specific effective correlation time which is sensitive to overall tumbling and slow (ns) time-scale internal motions. Details of the analysis are given in Choy et al.[9] Relaxation data were well fit using the spectral density function of eq 1, with χ^2 values not exceeding 10^{-4} for ^{15}N and reduced χ^2 values less than 3 for ^{2}H relaxation data.

In the LS-3 model, the motion of a bond vector is described by an autocorrelation function that decays rapidly to a plateau value with a correlation time τ_f, and then more gradually with a rate that depends on slow (ns) internal time-scale dynamics and overall tumbling (correlation time τ_c^{eff}). Although backbone and side chain dynamics in unfolded proteins are very likely to be more complicated, the limited number of measurables probing dynamics at only a small number of frequencies precludes the use of more complex models. Simulations show that if the methyl side chain dynamics consist of rapid (ps) internal motions (τ_f) and slower (ns) local dynamics (τ_s) with $\tau_f \ll \tau_s$ and $\tau_s >$ 2.5 ns, order parameter values (S^2_{axis}) extracted from the LS-3 model reflect the amplitude of the fast motions of the methyl symmetry axis. The effective correlation time, τ_c^{eff}, is in turn sensitive to the combined effects of slow local dynamics and overall tumbling. This model is discussed in some detail in a recent publication.[17] More complex models can very easily be constructed where the effects of ps and ns time-scale motions are clearly separated. However, we have shown that when errors in relaxation rates are taken into account in data fits, a wide range of dynamics parameters is often obtained for each methyl, even when errors in these rates are small and very comprehensive relaxation data sets are used. Further, the fits are no better than for the simpler LS-3 model.[16,17] We therefore prefer the LS-3 form of spectral density.

Fast Internal Motions. Side chain and backbone dynamics parameters extracted from the LS-3 model are listed in Table 1 and in Supporting Information, respectively. Interestingly, there are no dramatic changes in the order parameters at either backbone or side chain positions between pH 5.1 and 3.1, with changes of only 0.05 ± 0.04 and 0.03 ± 0.05 observed for side-chain methyls and backbone amides, respectively. This is consistent with similar amplitudes of fast time-scale dynamics for Δ131Δ at the two pH values.

To get a better physical picture of the side chain motions, in our previous work[9] we proposed that the S^2_{axis} values for Val

(14) Lipari, G.; Szabo, A. *J. Am. Chem. Soc.* **1982**, *104*, 4546−4559.
(15) Lipari, G.; Szabo, A. *J. Am. Chem. Soc.* **1982**, *104*, 4559−4570.
(16) Skrynnikov, N. R.; Millet, O.; Kay, L. E. *J. Am. Chem. Soc.* **2002**, *124*, 6449−6460.
(17) Choy, W. Y.; Kay, L. E. *J. Biomol. NMR* **2003**, *25*, 325−333.

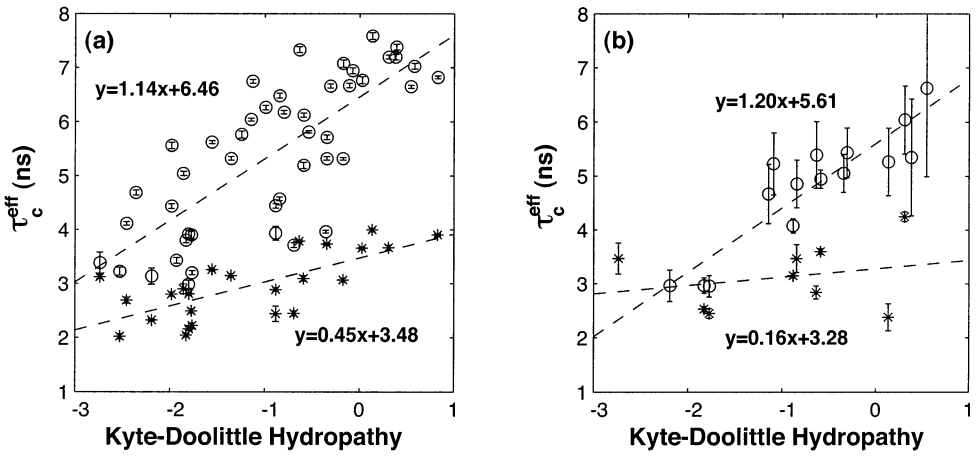

Figure 1. Plot of the effective correlation times of backbone $^1H-^{15}N$ bond vectors (a) and side chain methyl axes (b) in Δ131Δ at pH 5.1 (○) and 3.1 (∗) versus the Kyte−Doolittle hydropathy with window size of 11.

and Thr could be recast in terms of a model in which motion of the $C_\beta-C_\gamma$ bond is the sum of contributions from (i) backbone dynamics and (ii) χ_1 torsion angle fluctuations. The cone−GAF model, which combines wobbling-in-a-cone (backbone dynamics) and Gaussian axial fluctuations (χ_1 torsion angle fluctuations), can be used to estimate the amplitudes of χ_1 torsion angle fluctuations ($\sigma_{\chi 1}$) of Val and Thr on the basis of the backbone and side chain order parameters.[9] Assuming independence of wobbling-in-a-cone and χ_1 torsion angle fluctuations, S^2_{axis} can be expressed as:

$$S^2_{axis} = S^2_{C\beta-C\gamma} = \left(\frac{1}{192}\right) \left\{ \begin{array}{l} \sin^4(\beta)\,(7 + 4\cos\theta_o + \cos^2\theta_o)^2 \exp(-4{\sigma_{\chi_1}}^2) + \\ \sin^2(2\beta)\,(1 + 7\cos\theta_o + 4\cos^2\theta_o)^2 \exp(-{\sigma_{\chi_1}}^2) + \\ 12\,(3\cos^2(\beta) - 1)^2(\cos\theta_o + \cos^2\theta_o)^2 \end{array} \right\} \quad (2)$$

where β is equal to 180° minus the $C_\alpha-C_\beta-C_\gamma$ bond angle and θ_o is the semiangle of the cone in which the $C_\alpha-C_\beta$ bond wobbles uniformly. As a reasonable approximation, in the analysis of our data, we have substituted measured values of S^2_{NH} for $S^2_{C\alpha-C\beta}$.

The average $\sigma_{\chi 1}$ value for the six Val for which data could be obtained at pH 5.1 is 33.8°. To compare the amplitudes of χ_1 torsion angle fluctuations in this unfolded state to those in folded proteins, a database of side chain dynamics parameters for folded proteins obtained by ^2H spin relaxation measurements[18] has been analyzed using the cone−GAF model. For Val residues in the database, an average $\sigma_{\chi 1}$ value of 19.9 ± 10.6° was obtained. A similar mean $\sigma_{\chi 1}$ value (24.4°) based on ^3J-coupling constant data from nine Val in *Desulfovibrio vulgaris* flavodoxin has been estimated as well.[19] Thus, at least for valines, the average $\sigma_{\chi 1}$ value in Δ131Δ at pH 5.1 is approximately 10° larger than that observed for folded proteins. Notably, the average change in $\sigma_{\chi 1}$ between pH 5.1 and 3.1 for the four Val (V51, 74, 111, and 114) for which data is available at both pHs is very small, 3.2 ± 2.2°, on the order of experimental error. To put the increase in $\sigma_{\chi 1}$ values measured between folded and unfolded states in perspective, we have calculated $\sigma_{\chi 1}$ expected in the case of rapid (and equiprobable) interconversion between rotameric states for the Val residues mentioned above. Values of $\sigma_{\chi 1}$ on the order of 60° are predicted, 40° larger than in folded proteins. It is quite clear that on a ps time scale the extent of motions are much more limited, even in unfolded protein states.

The order parameter and $\sigma_{\chi 1}$ analysis described above suggests that decreasing the pH from 5 to 3 has little effect on the amplitudes of fast internal motions of the methyl side chains but that significant changes in amplitudes are noted upon transition from a folded to a largely unfolded state. The amplitudes of fast (ps) internal side chain motions are determined to a large extent by transitions within a given rotameric well. Thus, the increase in excursions (decreased order parameters) for a given methyl in an unfolded state relative to its folded counterpart likely reflect increases in the size of the well, with much smaller changes in well size between unfolded states of Δ131Δ at pH values of 5 and 3.

Slow Local Motions. The very small differences observed between order parameters obtained at pH = 5 and pH = 3 are consistent with a dynamical model in which the amplitudes of ps time-scale dynamics at both backbone and methyl side chain positions remain constant over this pH range. In contrast, τ_c^{eff} values are significantly decreased at the lower pH, by 38 ± 9 and 32 ± 14%, for backbone and side chain methyls respectively, illustrated in Figure 1. Simulations described previously show that decreases in τ_c^{eff} values extracted from the LS-3 model can be the result of increases in the amplitudes of slow local dynamics (such as segmental motion on the ns time scale).[17]

By means of example, we have simulated backbone ^{15}N relaxation data using a model for $J(\omega)$ which explicitly includes contributions from slow dynamics, developed by Clore and coworkers[16,20] using values of τ_f and S^2_{axis} of 100 ps and 0.6, respectively, along with a correlation time for slow local motions of 3 ns. Subsequently, the resulting rates have been fit with the LS-3 spectral density, eq 1. Values of τ_c^{eff} obtained from fits of these data using eq 1 are plotted as a function of the amplitude

(18) Mittermaier, A.; Kay, L. E.; Forman-Kay, J. D. *J. Biomol. NMR* **1999**, *13*, 181−185.
(19) Perez, C.; Lohr, F.; Ruterjans, H.; Schmidt, J. M. *J. Am. Chem. Soc.* **2001**, *123*, 7081−7093.
(20) Clore, G. M.; Szabo, A.; Bax, A.; Kay, L. E.; Driscoll, P. C.; Gronenborn, A. M. *J. Am. Chem. Soc.* **1990**, *112*, 4989−4991.

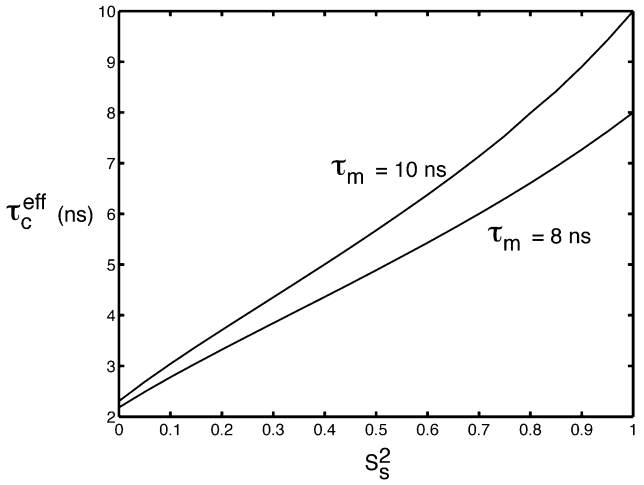

Figure 2. Plot of effective correlation times (τ_c^{eff}) extracted using the LS-3 model, eq 1, versus the input order parameters of the slow local motions (S_s^2) at two different overall tumbling times (τ_m = 8 and 10 ns). Error-free backbone ^{15}N R_1, R_2 and ^{1}H−^{15}N NOE data were simulated using a form of $J(\omega)$ described by Clore et al.,[16,20] which explicitly includes slow dynamics, assuming a spectrometer field of 800 MHz. In this model, the slow internal motions are parametrized by τ_s and S_s^2, the correlation time and the amplitude of the slow local dynamics. The simulated relaxation measurements (with τ_f, S_f^2 and τ_s set to 100 ps, 0.6 and 3 ns, respectively) were then fitted to the LS-3 model to extract τ_c^{eff}.

of the slow (ns) local motion (S_s^2) in Figure 2. In theory, as a protein losses residual contacts, the hydrodynamic radius of the molecule is expected to increase, leading to a larger overall tumbling time.[21,22] The simulations in Figure 2 show that an increase in the overall tumbling time alone (due to the expansion of the unfolded state ensemble from pH 5 to 3) would cause an increase in the τ_c^{eff}. Thus, the experimental observation of significant decreases in τ_c^{eff} values suggests substantial increases in the amplitudes of slow local motions upon lowering the pH.

We recognize that an alternative interpretation of the decrease in τ_c^{eff} at pH = 3 might be that at higher pH values Δ131Δ is partially aggregated (3.2 mM concentration), and that this association is reduced at lower pH due to the increase in net charge of the protein. The decreased aggregation would then account for the drop in ^{15}N R_2 values by approximately 30−35% observed for Δ131Δ at pH 3.1. However, Ohnishi and Shortle have recently reported a significant decrease (∼50% on average) of ^{15}N R_2 values in Δ131Δ upon lowering the pH from 5.2 to 3.0, using a much lower protein concentration of 1.2 mM.[23] An earlier SAXS study of a truncated form of SNase (deletion of residues 137−149 from the wild-type) has established that at this concentration, the protein is monomeric.[24] Thus, it is unlikely that the drop in ^{15}N R_2 values that we have observed, translating into decreased τ_c^{eff} values, is primarily the result of decreased aggregation at the lower pH, although we cannot rule out a small contribution from this effect.

Hydrophobic and Electrostatic Interactions in Δ131Δ. Recently, the profile of relaxation rates measured for reduced unfolded lysozyme, pH 2, and urea unfolded apomyoglobin, pH 2, have been interpreted in terms of hydrophobic contacts (lysozyme) and surface area burial upon folding (apomyoglobin).[25,26] In the case of Δ131Δ we observe a strong correlation of backbone and side chain methyl τ_c^{eff} values with the Kyte−Doolittle hydropathy[27] (which reflects the hydrophobicity of a residue's local environment) at pH 5 but a relatively weak correlation at pH 3 (Figure 1). It is well-known that protein stability is sensitive to environmental factors such as temperature, ionic strength, and pH. Δ131Δ has a high fraction of ionizable groups (∼40%) including six Asp and ten Glu and electrostatic interactions are expected to make a significant contribution to the stability of this unfolded protein fragment. Changes in the protonation states of Asp and Glu from pH 5 to 3 lead to dramatic changes in Coulombic interactions along the protein sequence with favorable interactions between basic and acidic groups at pH 5 disappearing at pH 3, where electrostatic repulsion between positively charged residues becomes dominant. This may lead to expansion of the unfolded state ensemble to reduce the strength of unfavorable charge−charge interactions. Thus, while the variation in amplitudes of the local ns motions of individual residues is likely determined primarily by residual hydrophobic contacts at pH 5, these interactions are overwhelmed by charge interactions in the pH 3 state, leading to an increase in the amplitudes of segmental motions and hence decreases in τ_c^{eff}.

In summary, the measured relaxation data are consistent with a picture in which librational motions on the ps time scale are enhanced in a "relatively structured" unfolded state of staphylococcal nuclease (Δ131Δ, pH 5), with $\sigma_{\chi 1}$ values on average 10° larger than in folded proteins (see above). Subsequent additional loss of structure (by decreasing the pH to 3) does not affect the amplitudes of these fast motions significantly. In contrast, hydrophobic contacts in the compact state at pH 5 are disrupted upon further destabilization of the protein when the pH is dropped to 3, leading to large amplitude motions on the ns time scale. The above study illustrates the utility of ^{15}N and ^{2}H spin relaxation experiments for probing residual structural interactions and dynamics in unfolded protein states.

Materials and Methods

Backbone and side chain relaxation measurements of Δ131Δ at pH 5.1 were reported in Choy et al.[9] All spin relaxation experiments at pH 3.1 were recorded on a 3.2 mM ^{15}N, ^{13}C, 50% ^{2}H-labeled sample of Δ131Δ, 1mM sodium azide, T = 32 °C (same concentration as for pH 5.1). Details of sample preparation are as given previously[10] with the exception that the protein was expressed in media containing 50% D_2O. The pH of the sample was adjusted to 3.1 by addition of concentrated HCl.

Backbone ^{15}N Relaxation Measurements. T_1, $T_{1\rho}$, and ^{1}H−^{15}N NOE experiments were recorded at 32 °C on a Varian Inova 800 MHz spectrometer. T_1 experiments were performed with eight relaxation delays, T, varying from 10 to 800 ms, while $T_{1\rho}$ experiments were recorded with eight relaxation delays between 10 and 100 ms, with a spin-lock field of 2 kHz. Steady-state ^{1}H−^{15}N NOE values were determined from intensity ratios of correlations in data sets recorded in the presence and absence of proton saturation. The NOE experiment utilized a 7 s relaxation delay followed by a 5 s period of saturation,

(21) Whitten, S. T.; Garcia-Moreno, E. B. *Biochemistry* **2000**, *39*, 14292−14304.
(22) Zhou, H. X. *Biophys. J.* **2003**, *83*, 2981−2986.
(23) Ohnishi, S.; Shortle, D. *Protein Sci.* **2003**, *12*, 1530−1537.
(24) Flanagan, J. M.; Kataoka, M.; Shortle, D.; Engelman, D. M. *Proc. Natl. Acad. Sci. U.S.A.* **1992**, *89*, 748−752.
(25) Klein-Seetharaman, J.; Oikawa, M.; Grimshaw, S. B.; Wirmer, J.; Duchardt, E.; Ueda, T.; Imoto, T.; Smith, L. J.; Dobson, C. M.; Schwalbe, H. *Science* **2002**, *295*, 1719−1722.
(26) Schwarzinger, S.; Wright, P. E.; Dyson, H. J. *Biochemistry* **2002**, *41*, 12681−12686.
(27) Kyte, J.; Doolittle, R. F. *J. Mol. Biol.* **1982**, *157*, 105−132.

while the NO−NOE spectrum was recorded in the absence of proton saturation with a relaxation delay of 12 s. All T_1, $T_{1\rho}$, and $^1H-^{15}N$ NOE spectra were recorded as 128 × 818 complex matrices with spectral widths of 1600.0 and 12775.5 Hz in the ^{15}N and ^1H dimensions, respectively, and processed and analyzed as described previously.[9]

Deuterium Relaxation Measurements. Deuterium spin relaxation experiments were recorded on a Varian Inova 800 MHz spectrometer, using pulse schemes described previously.[9] Each complex data set comprised 64 × 768 points, with spectral widths of 1400.0 and 12001.2 Hz in the ^{15}N and ^1H dimensions, respectively. For R_{D_Z}($R_{3D_Z^2-2}$) experiments the variable delay T was incremented from 0.5 to 50 ms (0.5−65 ms), while for R_{D_+} ($R_{D_+D_Z+D_ZD_+}$), delays ranged from 1 to 30 ms (1−50 ms). Sixteen transients/FID were signal averaged in the measurement of R_{D_Z} and R_{D_+}, while 32 scans were recorded for $R_{3D_Z^2-2}$ and $R_{D_+D_Z+D_ZD_+}$. Delays between scans of 2.0 s were employed.

Acknowledgment. Professor David Shortle (Johns Hopkins University), Dr. Satoshi Ohnishi (Johns Hopkins University), and Professor Huan-Xiang Zhou (Florida State University) are thanked for many useful discussions. W.-Y.C. is a recipient of a Senior Research Fellowship from the Canadian Institutes of Health Research (CIHR). This research was supported by a grant from the CIHR. L.E.K. holds a Canada Research Chair in Biochemistry.

Supporting Information Available: Table of backbone ^{15}N dynamical parameters of Δ131Δ measured at pH 5 and pH 3 (PDF). This material is available free of charge via the Internet at http://pubs.acs.org.

JA035705Q